International Conference on Space Optics—ICSO 2018

Chania, Greece

9–12 October 2018

Edited by Zoran Sodnik, Nikos Karafolas, and Bruno Cugny

Development of a low cost space telescope for Earth remote sensing from a 12U CubeSat

Helcio Vieira

Manoel N. Barcelos

International Conference on Space Optics — ICSO 2018, edited by Zoran Sodnik,
Nikos Karafolas, Bruno Cugny, Proc. of SPIE Vol. 11180, 111800Q · © 2018 ESA
and CNES · CCC code: 0277-786X/18/$18 · doi: 10.1117/12.2535945

Development of a Low-Cost Space Telescope for Earth Remote Sensing from a 12U CubeSat

Helcio Vieira Jr*[a], Manoel N. D. Barcelos Jr[a]
[a]University of Brasilia, Campus Universitario Darcy Ribeiro, Brasilia, Brazil

ABSTRACT

The purpose of this work is to develop a low-cost space telescope for Earth remote sensing that could be housed in a 12U CubeSat with a GSD of 25 meters at LWIR. It will be used the Three Mirror Anastigmatic concept and Commercial Off-The-Shelf components whenever it is possible.

The telescope main mission is the oil spill detection, mainly in ocean environment. Beyond the obvious functionality of this main mission, the oil spill detection can be very useful to detect crashed aircrafts in the ocean.

As secondary missions, this telescope can be used to map deforestation, finding lost ships in the ocean and help the drug smuggling by finding camouflaged man-made objects.

The Project current stage consists in preliminaries optical and mechanical projects in which the mirrors follow ITAR regulation.

The telescope will operate in LWIR frequencies and will extract polarization information from the target.

The preliminary optical project indicates that the telescope optical performance has Modulation Transfer Function greater than 45% at Nyquist frequency, native GSD of 25 meters and that the telescope is diffraction limited (wavefront error of 0.012 wavelengths and Strehl ratio of 99.38%).

The preliminary mechanical project indicates that the maximum deflection caused by gravity induces to a despicable error (smaller than one over one hundred and forty) when compared to the mean wavelength of operation.

The preliminary radiometric analyses indicates that the telescope has a NETD of 0.90 K.

Keywords: Remote Sensing, LWIR, CubeSat, Polarimetric

1. INTRODUCTION

The purpose of this work is to develop a low-cost space telescope for Earth remote sensing that could be housed in a 12U CubeSat with a GSD of 25 meters at LWIR. It will be used the Three Mirror Anastigmatic concept and Commercial Off-The-Shelf components whenever it is possible.

The telescope main mission is the oil spill detection, mainly in ocean environment. Beyond the obvious functionality of this main mission, the oil spill detection can be very useful to detect crashed aircrafts in the ocean (as the accident of the Air France 447, flying between Rio de Janeiro, Brazil, and Paris, France, which crashed at May 31, 2009).

As secondary missions, this telescope can be used to map deforestation, finding lost ships in the ocean and help the drug smuggling by finding camouflaged man-made objects.

The telescope will operate in LWIR frequencies and will extract polarization information from the target.

The motivation for the initial choices we made for the project variables are the following:

- **Infrared:** the greater the operation frequency, the greater will be the acceptable tolerances in the mirrors manufacturing and in their assembly. As one of the objectives of this project is the low cost of the final product, having greater tolerances will decrease the final cost of the telescope.

*helciovj@unb.br; phone 55 61 993794605

The sensor will be based on the microbolometer technology. This type of sensor does not need refrigeration, which, besides decreasing the cost and complexity of the project, decreases the volume of the telescope. One of the objectives of this project is that the telescope could be housed in a CubeSat greater than the standard 12U.

- **Polarized**: the use of polarimetry increases the probability of oil spill identification in water[1]. Fig. 1 illustrates this concept.

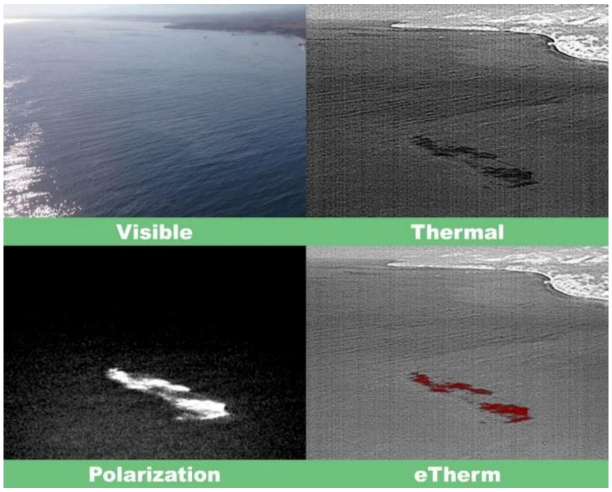

Figure 1. Polarimetry utilization for oil spill identification. Source: Ref. 2.

Besides that, the polarimetry utilization helps in the identification of man-made objects, as can be seen in Fig. 2.

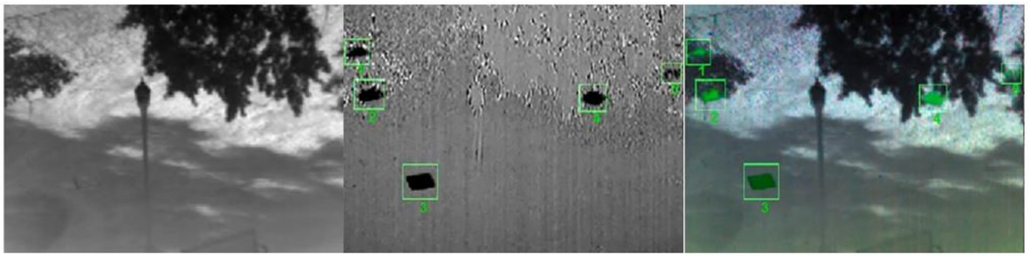

Figure 2. Images: thermal (left), polarimetric (center), and e-therm (right). Source: Ref. 2.

The available solutions to measure polarization can be classified as[3]: (a) spatial domain, like beam-splitters and microgrid polarizer arrays; (b) temporal domain, like rotating polarizers and rotating retarders; and (c) spectral domain, like channeled spectropolarimeters. We opted to use a microgrid polarizer array, such the one illustrated in Fig. 3.

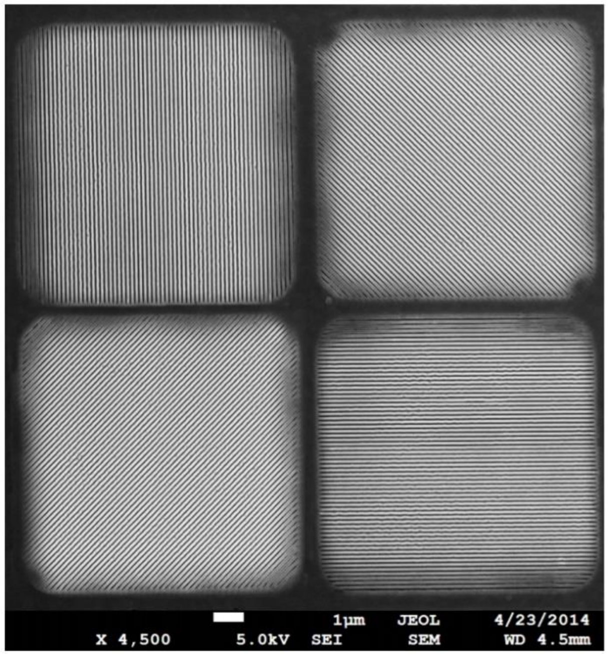

Figure 3. Image of four pixels of a micropolarizer array. Source: Ref. 3.

- **All-metallic**: The use of only one substrate for the mirrors and the structure minimizes the optical distortion problem due to temperature changes. Ref. 4 states that an aluminum all-metallic project (as the one described in this document) is quasi-athermal.

The remaining of this paper is organized as follows. Section II describes the telescope project and its current stage. The next steps to finish the project will be listed in Section III. Finally, we conclude in Section IV.

2. THE PROJECT

The current stage of this work consists in preliminaries optical and mechanical projects in which the mirrors follow ITAR regulation. The ITAR regulation constrains the maximum aperture stop of the optics allowable to be exported to be smaller than 50 cm[5].

2.1 Preliminary Optical Project

The preliminary optical project took as hypotheses a focal plane array (FPA) with pixel pitch p of 17 microns, a wavelength λ ranging from 7.5 to 13.5 microns, a flight altitude H of 450 km, an aperture stop D of 187.5 mm and a focal length f of 306 mm. These data lead to the following values of GSD (ground sampling distance) and GRD (ground resolution distance):

$$GSD = \frac{pH}{f} = 25 \text{ m} \tag{1}$$

$$GRD = 1.22\frac{\lambda H}{D} = 30.74\text{m} \tag{2}$$

The GSD equals the FPA pixel projection on the ground. Fig. 4 illustrates this concept, where IGFOV represents the GSD.

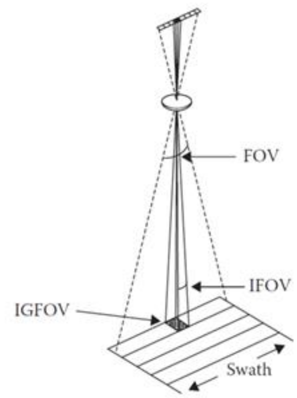

Figure 4. Pixel projection on the ground. Source: Ref. 6.

The GRD corresponds to the Rayleigh resolution criterion[6]. Rayleigh proposed that two objects are resolved when the maximum of the diffraction pattern of the first corresponds to the first minimum of the second, as illustrated by Fig. 5.

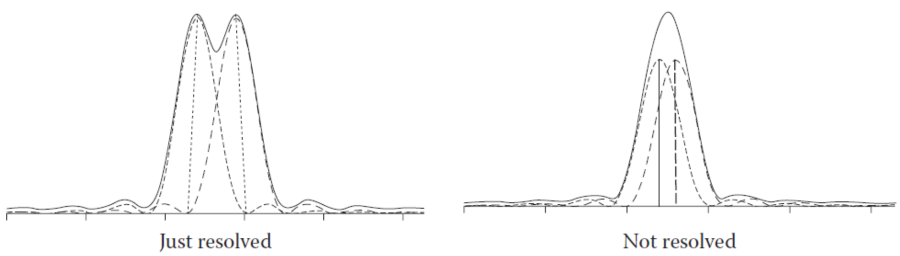

Figure 5. GRD concept. Source: Ref. 6.

In the preliminary optical project, the rate $GRD/GSD = 1.23$. Table 1 lists data from several operational satellites so the rate GRD/GSD can be analyzed. In this table, the columns named *GSD* and *GRD* were calculated using equations (1) and (2), and the column *nominal GSD* indicates the advertised GSD by the satellite operator.

Table 1. Data from several operational satellites. All units are meters. Source: Ref. 6.

Satellite	*H*	*D*	*f*	*p*	λ	Nominal GSD	GSD	GRD	GRD/GSD
SPOT1-4	828.000	0,31	1,08	1,30E-05	6,15E-07	10,000	9,967	2,004	0,201
SPOT5	828.000	0,31	1,08	4,60E-06	6,15E-07	3,500	3,527	2,004	0,568
RESUSDK1	350.000	0,50	4,00	9,00E-06	6,75E-07	1,000	0,788	0,576	0,732
ORBVIEW3	470.000	0,45	2,77	5,40E-06	6,75E-07	1,000	0,916	0,860	0,939
CARTOSAT2A	635.000	0,70	5,60	7,00E-06	6,75E-07	0,800	0,794	0,747	0,941
KOMPSAT2	685.000	0,60	9,00	1,30E-05	6,75E-07	1,000	0,989	0,940	0,950
IKONOS2	681.000	0,70	10,00	1,20E-05	6,75E-07	0,820	0,817	0,801	0,980
QUICKBIRD2	450.000	0,60	8,80	1,20E-05	6,75E-07	0,610	0,614	0,618	1,007
EROSB	510.000	0,50	5,00	7,00E-06	6,75E-07	0,700	0,714	0,840	1,176
PLEIADES1	694.000	0,65	12,90	1,30E-05	6,55E-07	0,700	0,699	0,853	1,220
GEOEYE1	684.000	1,10	13,30	8,00E-06	6,75E-07	0,410	0,411	0,512	1,245
WORLDVIEW2	770.000	1,10	13,30	8,00E-06	6,75E-07	0,460	0,463	0,576	1,245
WORLDVIEW1	496.000	0,60	8,80	8,00E-06	6,75E-07	0,450	0,451	0,681	1,510

The satellites in in the hatched area of Table 1 are the ones in which the rate $GRD/GSD > 1$ and their average value is 1.23. The rate GRD/GSD of our project being the average value of several operational satellites shows that the nominal performance of the preliminary optical project is completely feasible to be achieved.

Fig. 5 shows the preliminary optical project.

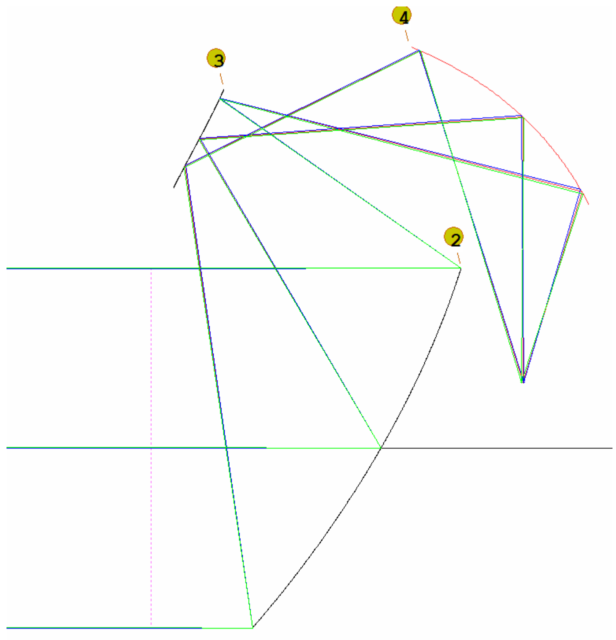

Figure 6. Preliminary optical project.

The preliminary optical project indicates that the telescope optical performance has Modulation Transfer Function[7] greater than 45% at Nyquist frequency, as shown in Fig. 7, native GSD of 25 meters and that the telescope is diffraction limited (wavefront error of 0.012 wavelengths and Strehl ratio of 99.38%).

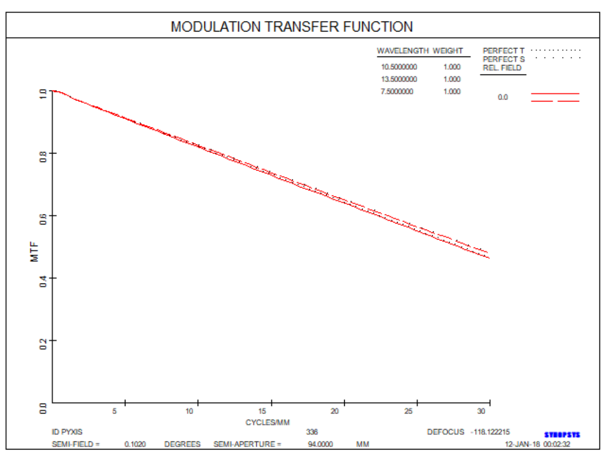

Figure 7. Modulation Transfer Function.

In order to achieve this performance, we designed the mirrors to be free-form ones, described by Zernike polinomials[8] of order up to 36th.

2.2 Radiometric Considerations

Ref. 9 defines the noise equivalent temperature difference (NEΔT or NETD) as the temperature difference between a target and the background that produces a signal equivalent to the noise. They state NETD is directly proportional to the square of the F-number (f/#) and is inversely proportional to the incident radiation.

The thermal response time τ, also known as time constant, "expresses the physical time a bolometer needs to heat up and give an electrical output that equals or represents the input" [10]. Ref. 11 states that there is a NETD/τ proportionality relationship and that it is accurate since the NETD is limited by 1/f noise. After 3τ, which is the usual time the FPA manufactures use as integration time, the output signal will represent 95% of the input signal[10].

A Time Delay Integration (TDI) is an artifact that improves the SNR by a factor of $\sqrt{N}$, where N is the number of stages[6].

For a telescope flying at 450 km of altitude, the dwell time of a ground resolution cell of 25 m is 3.5 ms. Setting the integration time to this value will produce an image with minimum motion blur.

We assume a commercial microbolometer FPA[12] (thermal response time of 14 ms and NETD of 40 mK at f/# =1.0) and the optics described at 2.1 with f/# = f/D = 1.632. Given the NETD/τ proportionality relationship[11], it is possible to achieve, with the same technology of this commercial microbolometer, a FPA with thermal response time of 1.17 ms and NETD of 480.0 mK (14.0 x 40.0 = 1.17 x 480.0). The optics make the NETD to be 1278.44 mK. Assuming the polarization filter will divide the signal into 4 equal parts, then NETD = 5113.77 mK. Finally, with a TDI of 32 stages, we will have a NETD of 0.90 K.

In this fashion, we propose a FPA with fast thermal response time (3 x 1.17 ms = 3.5 ms = 25 m GSD) and 32 stages of TDI, as illustrated in Fig. 8, where each block of same polarization has 640 columns by 8 lines.

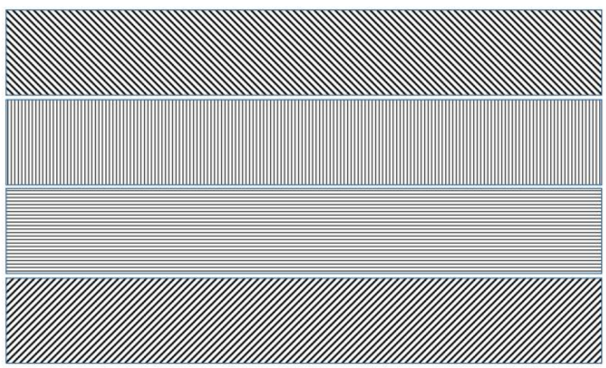

Figure 8. Projected micropolarizer pattern.

2.3 Preliminary Mechanical Project

We opted to use aerospace qualified aluminum (Al6061-T6) as subtract to both mirrors and structure. The reasons that drove this decision were the same ones listed by Ref 13: "Al6061-T6, which is diamond turnable but also offers distinguished optical quality for IR-optics, especially if fine grain sized aluminum alloy like RSA-6061 is used".

The preliminary mechanical project, added by the light rays, is shown in Fig. 9, where the mirrors are painted in dark gray, the light rays in blue and the structure in light gray.

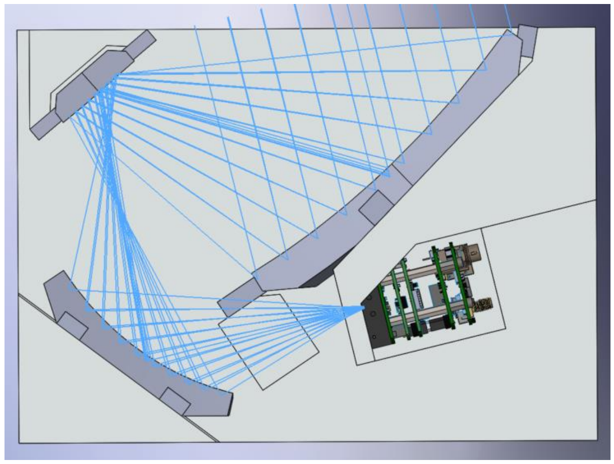

Figure 9. Preliminary mechanical project.

Fig. 10 shows three perspective visions from the mechanical project.

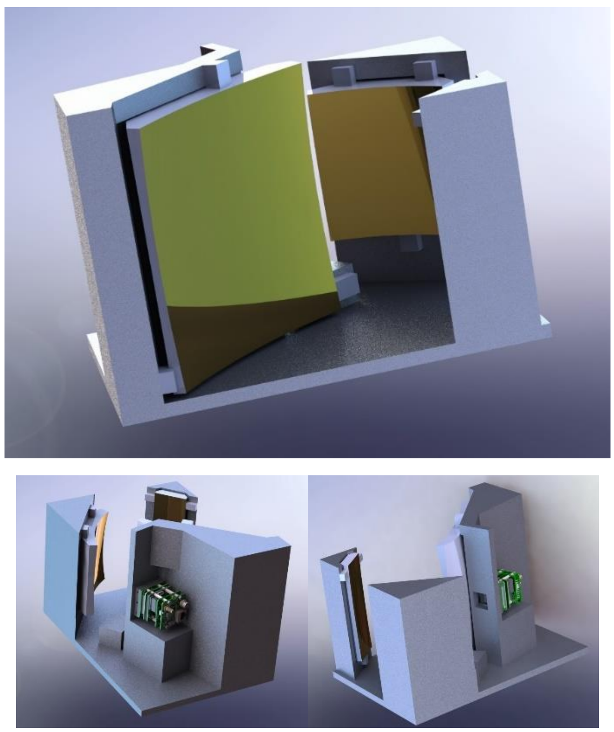

Figure 10. Perspective visions from the mechanical project.

It was done a study on the mechanical project through finite element method[8]. The result of this study is shown in Fig. 11 and Fig. 12, where the maximum deflection δ caused by gravity is smaller than 74 nanometers. This deflection induces to a despicable error (smaller than one over one hundred and forty) when compared to the mean wavelength of operation ($\lambda = 10.5$ microns).

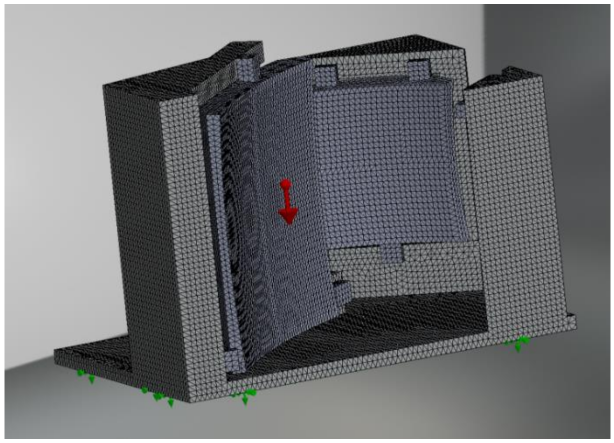

Figure 11. Mesh generated for the finite element analysis.

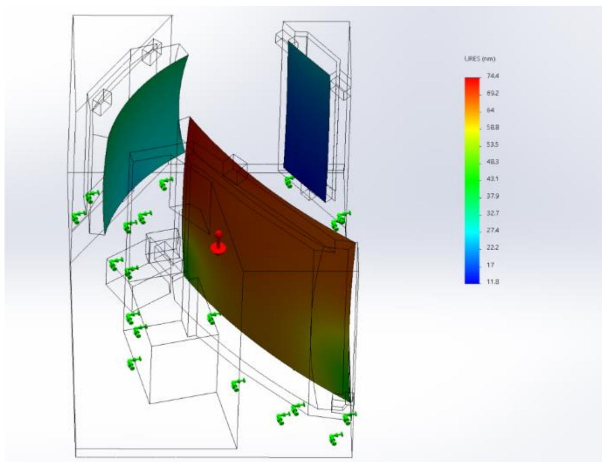

Figure 12. Static analysis done by finite element method for the deflection caused by gravity.

3. NEXT STEPS

It must be frozen the optical and mechanical projects. In order to do that, it is necessary to perform the following critical actions, among others:

- Frozen the FPA to be utilized: this step is essential to allow the next one (radiometric analysis);
- Do the radiometric analysis: this is the most critical step. The reason is that it could not exist a microbolometer FPA with line rate and response time fast enough to allow the desired GSD with an acceptable NETD. If this will be the case, our alternative would be increasing the pixel pitch and also the GSD;
- Do the sensitivity analysis on the optical project: it will allow the procurement of the mirrors;
- Finish the static analysis on the mechanical project;
- Do the frequency response analysis on the mechanical project: this analysis will show if there will be restrictions on what type of launchers (rockets) could be used to orbit this sensor;
- Do the thermal analysis on both optical and mechanical projects: it will show how many thermostat and heaters will be necessary to maintain the telescope without thermal gradients. It will also furnish the estimate of power consumption of the sensor;

After these steps, we foresee the following phases to conclude the project:

- Procure mirror manufacturer;
- structure manufacturer;
- Acquire the FPA;
- Align the mirrors;
- Measure the telescope performance.

4. CONCLUSION

The purpose of this work is to develop a low-cost space telescope for Earth remote sensing that could be housed in a 12U CubeSat with a GSD of 25 meters at LWIR. It was used the Three Mirror Anastigmatic concept and Commercial Off-The-Shelf components whenever it is possible.

Section II described the telescope project and its current stage and the next steps to finish the project were listed in Section III.

The telescope main mission is the oil spill detection, mainly in ocean environment. Beyond the obvious functionality of this main mission, the oil spill detection can be very useful to detect crashed aircrafts in the ocean.

As secondary missions, this telescope can be used to map deforestation, finding lost ships in the ocean and help the drug smuggling by finding camouflaged man-made objects.

The Project current stage consists in preliminaries optical and mechanical projects in which the mirrors follow ITAR regulation.

The telescope will operate in LWIR frequencies and will extract polarization information from the target.

It could be seen that the preliminary optical project indicated that the telescope optical performance has Modulation Transfer Function greater than 45% at Nyquist frequency, native GSD of 25 meters and that the telescope is diffraction limited (wavefront error of 0.012 wavelengths and Strehl ratio of 99.38%).

The preliminary mechanical project indicated that the maximum deflection caused by gravity induces to a despicable error (smaller than one over one hundred and forty) when compared to the mean wavelength of operation. The preliminary radiometric analyses indicated that the telescope has a NETD of 0.90 K.

We are still in the very beginning of this project, but the results we have so far strongly support our believe that the fulfillment of our goals is feasible.

5. ACKNOWLEDGMENTS

We would like to thank the Fundacao de Apoio a Pesquisa do Distrito Federal (FAP-DF) for its financial support.

6. REFERENCES

[1] Chenault, D. B., Vaden, J., Mitchell, D., and Demicco, E., “New IR polarimeter for improved detection of oil on water.” SPIE Newsroom. http://www.polarissensor.com/app/uploads/2017/05/SPIE-Pyxis-Joint-Exxon-Article.pdf. (Accessed: January 12, 2018).

[2] Polaris, “Oil and diesel on water.” Unpublished. http://www.polarissensor.com/applications/water-detection/oil-and-diesel/. (Accessed: January 12, 2018).

[3] Snik, F., Craven-Jones, J., Escuti, M., Fineschi, S., Harrington, D., Martino, A. D., Mawet, D., Riedi, J.,and Tyo, J. S., “An overview of polarimetric sensing techniques and technology with applications to different research fields,” in [Proc. of SPIE], 9099 (2014).

[4] Kirschstein, S., Koch, A., Schoneich, J., and Dongi, F., "Metal mirror TMA, telescopes of the JSS product line: design and analysis," in [Proc. of SPIE], 1939 (1993).

[5] USA State Department, "US Munitions List - ITAR Control." Unpublished. https://www.ecfr.gov/cgi-bin/text-idx?SID=86008bdffd1fb2e79cc5df41a180750a&node=22:1.0.1.13.58&rgn=div5. (Accessed: January 23, 2018).

[6] Joseph, G., [Building Earth Observation Cameras], CRC Press (2015).

[7] Smith, G. H., [Practical Computer-Aided Lens Design], Willmann-Bell (1998).

[8] Andersen, T. and Enmark, A., [Integrated Modeling of Telescopes], Springer (2011).

[9] Redjimi, A., Knezevic, D., Savic, K., Jovanovic, N., Simovic, M., and Vasiljevic, D., "Noise Equivalent Temperature Difference Model for Thermal Imagers, Calculation and Analysis." Unpublished. http://www.vti.mod.gov.rs/ntp/rad2014/2-2014/6/6.pdf. (Accessed: January 29, 2018).

[10] Xenics Infrared Solutions, "What is the thermal time constant?." Unpublished. http://www.xenics.com/en/faq/what-thermal-time-constant. (Accessed: January 27, 2018).

[11] Kohin, M. and Butler, N., "Performance limits of uncooled vox microbolometer focal plane arrays," in [Proc. of SPIE], 5406 (2004).

[12] DRS Technologies, "U8000." Unpublished. http://www.drsinfrared.com/portals/0/docs/datasheets/U8000_MR-2012-04-618_Rev02.pdf. (Accessed: February 02, 2018).

[13] Scheiding, S., Damm, C., Holota, W., Peschel, T., Gebhardt, A., Risse, S., and Tnnermann, A., "A ultraprecisely manufactured mirror assemblies with well defined reference structures," in [Proc. of SPIE], 7739,D1–D10 (2010).